Journal of Theoretical Biology 450 (2018) 30–36

Contents lists available at ScienceDirect

Journal of Theoretical Biology

journal homepage: www.elsevier.com/locate/jtbi

A guideline to study the feasibility domain of multi-trophic and changing ecological communities

Chuliang Song[a], Rudolf P. Rohr[b], Serguei Saavedra[a,1,*]

[a] Department of Civil and Environmental Engineering, MIT, 77 Massachusetts Av., Cambridge, MA 02139, USA
[b] Department of Biology - Ecology and Evolution, University of Fribourg Chemin du Musée 10, Fribourg CH-1700, Switzerland

ARTICLE INFO

Article history:
Received 16 October 2017
Revised 18 April 2018
Accepted 19 April 2018
Available online 24 April 2018

Keywords:
Convex geometry
Feasibility domain
Species interactions
Population dynamics
Trophic energy flow

ABSTRACT

The feasibility domain of an ecological community can be described by the set of environmental abiotic and biotic conditions under which all co-occurring and interacting species in a given site and time can have positive abundances. Mathematically, the feasibility domain corresponds to the parameter space compatible with positive (feasible) solutions at equilibrium for all the state variables in a system under a given model of population dynamics. Under specific dynamics, the existence of a feasible equilibrium is a necessary condition for species persistence regardless of whether the feasible equilibrium is dynamically stable or not. Thus, the size of the feasibility domain can also be used as an indicator of the tolerance of a community to random environmental variations. This has motivated a rich research agenda to estimate the feasibility domain of ecological communities. However, these methodologies typically assume that species interactions are static, or that input and output energy flows on each trophic level are unconstrained. Yet, this is different to how communities behave in nature. Here, we present a step-by-step quantitative guideline providing illustrative examples, computational code, and mathematical proofs to study systematically the feasibility domain of ecological communities under changes of interspecific interactions and subject to different constraints on the trophic energy flows. This guideline covers multi-trophic communities that can be formed by any type of interspecific interactions. Importantly, we show that the relative size of the feasibility domain can significantly change as a function of the biological information taken into consideration. We believe that the availability of these methods can allow us to increase our understanding about the limits at which ecological communities may no longer tolerate further environmental perturbations, and can facilitate a stronger integration of theoretical and empirical research.

1. Introduction

In ecological research, the feasibility of a community corresponds to the existence of an equilibrium point under which all species have positive abundances (Case, 2000; Hofbauer and Sigmund, 1998; MacArthur, 1970; Meszéna et al., 2006; Pimm, 1982; Roberts, 1974). Indeed, if one is interested in extant species, negative or zero abundances make no biological sense. Therefore, studying the feasibility of an ecological community is equal to determining whether under a given set of environmental conditions (abiotic and biotic) the dynamics of a community exhibits a feasible equilibrium point. That is, feasibility is a binary question: a community is feasible or not under a given set of environmental conditions. Nevertheless, one can also extend the study of feasibility by investigating the range of environmental conditions leading to a feasible community. This specific range of environmental conditions is known as the *feasibility domain* (Logofet, 1993). Thus, the size of the feasibility domain can be used as an indicator of the tolerance of a community to random environmental variations (Rohr et al., 2016; Saavedra et al., 2014). This has motivated a rich research agenda to estimate the feasibility of ecological communities in a systematic manner (Bastolla et al., 2009; Gilpin, 1975; Goh and Jennings, 1977; Grilli et al., 2017; Logofet, 1993; Meszéna et al., 2006; Rohr et al., 2014; Saavedra et al., 2017b; Stone, 2016; Vandermeer, 1975). Yet, it is still unclear how to integrate this systematic analysis with additional biological information, such as differences in energy flows across trophic levels or even changes in the structure of ecological communities.

Here, we present a step-by-step quantitative guideline to study the size of the feasibility domain of ecological communities under

* Corresponding author.
E-mail address: sersaa@mit.edu (S. Saavedra).
[1] ORCID 0000-0003-1768-363X

https://doi.org/10.1016/j.jtbi.2018.04.030
0022-5193/

changes of interspecific interactions and subject to different constraints on the trophic energy flows. This guideline covers multitrophic communities that can be formed by any type of interspecific interactions. While our framework is based on the classic Lotka-Volterra (LV) dynamics (Page and Nowak, 2002), its advantage is that the structure and limits of the feasible regions of a large variety of ecological communities can be systematically studied using convex geometry and probability theory (Ball, 1997; Brondsted, 2012; Logofet, 1993; Rohr et al., 2014). Moreover, the applicability of this approach is not restricted to LV dynamics as long as the dynamics are topologically equivalent (Cenci and Saavedra, 2018).

This article is organized as follows. First, we discuss the mathematical definition, geometrical representation, and the probabilistic interpretation of the feasibility domain in multispecies communities characterized by LV dynamics. Then, we introduce new tools to incorporate both changes of species interactions and trophic energy constraints into the study of feasibility. After that we present an illustrative example to show how our tools can be applied to multi-trophic and changing communities. Finally, we discuss future promising avenues of research on feasibility. While we present an abridged guideline in the text, all the proofs can be found in the Appendixes A–E, and the computational codes in R Core Team (2017) is archived on Github.

2. Mathematical definition of feasibility

We start by assuming that the population dynamics in a multispecies community can be approximated by a LV system in the form

$$\frac{dN_i}{dt} = N_i\left(r_i + \sum_{j=1}^{S} a_{ij}N_j\right), \tag{1}$$

where the variable N_i denotes the abundance of species i, S is the number of species, the parameter r_i is the intrinsic growth rate of species i, and the parameter a_{ij} is the element (i, j) of the interaction matrix $\boldsymbol{A}$ and represents the effect of species j on species i (Case, 2000). Note that both the intrinsic growth rates and the elements of the interaction matrix can take either positive, negative, or zero values. We take into account only non-degenerate interaction matrices, i.e., $\det(\boldsymbol{A}) \neq 0$. This assumption is valid since it is extremely rare to have degenerate cases even under the setup of random matrix theory (Bruneau and Germinet, 2009).

Under the LV dynamics, the equilibrium state(s) of the population is(are) written as the vector $\boldsymbol{N}^*$, which corresponds to the state at which $dN_i/dt = 0$ for all species i. This equilibrium state(s) is(are) given by the solution(s) of the set of equations

$$N_i^*\left(r_i + \sum_{j=1}^{S} a_{ij}N_j^*\right) = 0. \tag{2}$$

The positivity of LV dynamics, i.e., species abundances will never be negative with strictly positive initial conditions, imposes two types of equilibria (Takeuchi, 1996). There can be either a border equilibrium, where at least a species goes extinct ($N_i^* = 0$ for some species i), or a *feasible* equilibrium (also known as *interior* equilibrium), where all species have positive abundances ($\boldsymbol{N}^* > 0$). If the feasible equilibrium exists is given by $\boldsymbol{N}^* = -\boldsymbol{A}^{-1}\cdot\boldsymbol{r}$. Moreover, one can mathematically prove that for a LV model, the existence of a feasible equilibrium point is a necessary condition for species persistence (and permanence), whether that feasible equilibrium is dynamically stable or not (Hofbauer and Sigmund, 1998).

The mathematical definition above reveals that feasibility depends strictly on the elements of both the interaction matrix $\boldsymbol{A}$ and the vector of intrinsic growth rates $\boldsymbol{r}$ (Song and Saavedra, 2018). This implies that, given an interaction matrix $\boldsymbol{A}$, only certain combinations of species-specific intrinsic growth rates can generate feasible equilibria, i.e., for which we have $-\boldsymbol{A}^{-1}\cdot\boldsymbol{r} > 0$. Following this rationale, studies have been systematically investigating the feasibility of ecological communities by looking at the range of parameter values of $\boldsymbol{r}$ as a function of a given interaction matrix $\boldsymbol{A}$ (Bastolla et al., 2009; Grilli et al., 2017; Logofet, 1993; Rohr et al., 2014; Saavedra et al., 2017b; Vandermeer, 1975). Importantly, since environmental conditions can be translated into the vital rates of species (Coulson et al., 2017; Levins, 1968; Meszéna et al., 2006; Roughgarden, 1975), the range of intrinsic growth rates leading to feasibility can represent a set of environmental variations tolerated by the community.

3. Geometrical representation of feasibility

As explained above, there is only a specific region of the parameter space of intrinsic growth rates that leads to feasible equilibria of a community given by an interaction matrix $\boldsymbol{A}$. This region is typically known as the *feasibility domain* (Logofet, 1993). Formally, this feasibility domain is described as

$$D_F(\boldsymbol{A}) = \{\boldsymbol{r} = N_1^*\boldsymbol{v}_1 + \cdots + N_S^*\boldsymbol{v}_S, \text{ with } N_1^* > 0, \ldots, N_n^* > 0\}, \tag{3}$$

where the vector $\boldsymbol{v}_j$ is the negative of the jth columns of the interaction matrix $\boldsymbol{A}$:

$$\boldsymbol{A} = \begin{bmatrix} a_{11} & \cdots & a_{1S} \\ \vdots & \ddots & \vdots \\ a_{S1} & \cdots & a_{SS} \end{bmatrix} = \begin{bmatrix} \vdots & \vdots & & \vdots \\ -\boldsymbol{v}_1 & -\boldsymbol{v}_2 & \ldots & -\boldsymbol{v}_S \\ \vdots & \vdots & & \vdots \end{bmatrix}. \tag{4}$$

In other terms, the vectors of intrinsic growth rates inside the feasibility domain are described by positive linear combinations of the S vectors given by the negative of each of the S columns of the interaction matrix (see Appendix A for further details).

This definition implies that the feasibility domain, $D_F(\boldsymbol{A})$, of an interaction matrix $\boldsymbol{A}$ can be geometrically represented as an algebraic cone (see Fig. 1a for a graphical illustration). An algebraic cone in $\mathbb{R}^S$ is defined as the space spanned by positive linear combinations of S linearly independent vectors. This cone is also referred in the mathematical literature as a *simplicial cone* (Ribando, 2006). For brevity, we will refer to it simply as a *cone*. Therefore, $\boldsymbol{v}_i$ can be defined as the i^{th} spanning vector of the feasible cone. This geometric property confirms, as we mentioned before, that the shape and size of the feasibility domain can be systematically investigated using convex geometry and probability theory (Ball, 1997; Brondsted, 2012; Logofet, 1993).

4. Probabilistic interpretation of feasibility

The definitions above allow us to quantify the size of the feasibility domain under LV dynamics by the solid angle of the cone generated by the interaction matrix $\mathbf{A}$ (see Fig. 1b for a graphical illustration). By normalizing the solid angle such that it is equal to one for the whole unit sphere in $\mathbb{R}^S$, the normalized solid angle $\Omega(\mathbf{A})$ is equal to the probability of sampling uniformly a vector of intrinsic growth rates on the unit sphere inside the feasibility domain. That is, the normalized solid angle is the proportion of the feasible parameter space inside the unit sphere. Formally, the normalized solid angle $\Omega(\mathbf{A})$ can be defined by the ratio of the following volumes:

$$\Omega(\boldsymbol{A}) = \frac{\text{vol}(D_F(\boldsymbol{A}) \cap \mathbb{B}^S)}{\text{vol}(\mathbb{B}^S)}, \tag{5}$$

where $\mathbb{B}^S$ is the closed unit ball in dimension S (Gourion and Seeger, 2010; Saavedra et al., 2016a). Note that the least upper bound of $\Omega(\boldsymbol{A})$ is 0.5, as the largest cone that can be generated by

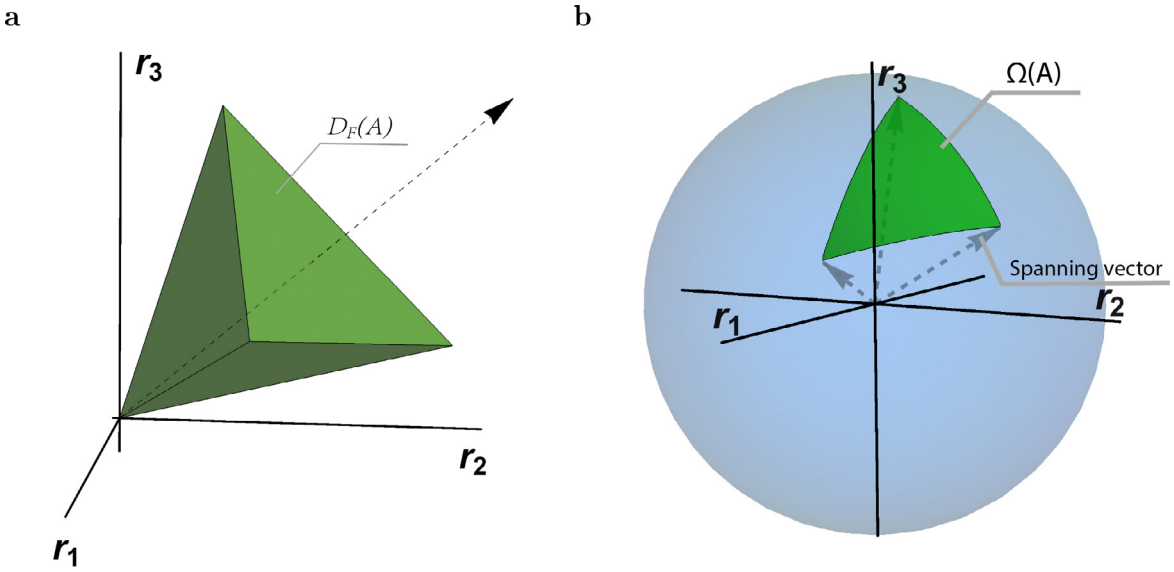

Fig. 1. Visualization of the feasibility domain and its normalized solid angle. For a fictitious community of three species represented by an interaction matrix $\boldsymbol{A}$ with all negative entries, the figures correspond to the parameter space of intrinsic growth rates ($\boldsymbol{r} = [r_1, r_2, r_3]^{\mathrm{T}}$). In Panel **a**, the green cone represents the feasibility domain $D_F(\boldsymbol{A})$ generated by the negative column vectors (spanning vectors) of the interaction matrix $\boldsymbol{A}$ (see Eq. (3)). The arrow corresponds to a hypothetical vector of intrinsic growth rates inside the feasibility domain. In Panel **b**, the blue unit sphere corresponds to the normalized parameter space. The normalized solid angle of the feasible cone $\Omega(\boldsymbol{A})$ corresponds to the fraction of the volume in the unit sphere occupied by the cone (green region), which can be interpreted as tolerance of a community to random environmental perturbations. (For interpretation of the references to color in this figure legend, the reader is referred to the web version of this article.)

an interaction matrix is exactly given by the half of the parameter space (see Appendix B for the mathematical derivation). Therefore, the closer $\Omega(\boldsymbol{A})$ is to 0.5, the larger the likelihood of randomly sampling a feasible community for a given interaction matrix $\boldsymbol{A}$.

Analytically, $\Omega(\boldsymbol{A})$ can be calculated by the cumulative function of a multivariate Gaussian distribution (Ribando, 2006; Saavedra et al., 2016b):

$$\Omega(\boldsymbol{A}) = \frac{1}{(2\pi)^{S/2}\sqrt{|\det(\boldsymbol{A})|}} \int \cdots \int_{\boldsymbol{N^*}\geq 0} e^{-\frac{1}{2}\boldsymbol{N^*}^{\mathrm{T}}\boldsymbol{A}^{\mathrm{T}}\boldsymbol{A}\boldsymbol{N^*}}\, \mathrm{d}\,\boldsymbol{N^*}, \tag{6}$$

This normalized solid angle $\Omega(\boldsymbol{A})$ can be efficiently computed via a quasi-Monte Carlo method for even relatively large communities (Genz and Bretz, 2002; Saavedra et al., 2016b). The code in R to compute this probability is archived on GitHub. Note that there exists a close analytic formula to compute the expectation of $\Omega(\boldsymbol{A})$ for independent and identically distributed (i.i.d.) random matrices $\boldsymbol{A}$, i.e., where each element of these matrices is drawn independently from the same statistical distribution (Grilli et al., 2017).

Another important probabilistic interpretation of the feasibility domain can be derived by calculating the average probability $\omega(\boldsymbol{A})$ that a randomly chosen species i from a given community is feasible (i.e., $N_i^* > 0$). Assuming that this choice is i.i.d. for all species, which can be valid when the coupling of interactions is not too strong in the community (Sugihara et al., 2012), we compute $\omega(\boldsymbol{A})$ as $\omega(\boldsymbol{A}) = \Omega(\boldsymbol{A})^{1/S}$. Indeed, the product of the average probability $\omega(\boldsymbol{A})$ across all species in the community has to equal the size of the feasibility domain of the whole community, i.e., $\omega(\boldsymbol{A})^S = \Omega(\boldsymbol{A})$. In other words, $\omega(\boldsymbol{A})$ translates the probabilistic interpretation of feasibility from the community to the species level.

In the hypothetical case where all species in a community do not interact (i.e., the interaction matrix becomes $\boldsymbol{A} = \boldsymbol{H} = \mathrm{diag}\{h_1, \ldots, h_S\} < 0$), we have $\omega(\boldsymbol{H}) = 0.5$. Indeed, for the whole community to be feasible there must be $r_i > 0$ for all species. Therefore, the size of the feasibility domain is given by the strictly positive part of the parameter space, i.e., $D_F(\boldsymbol{H}) = \mathbb{R}^S_{>0}$, which has the normalized solid angle of $\Omega(\boldsymbol{H}) = 0.5^S$. This is equivalent to say that the probability that any of the species in the community has positive abundance at equilibrium is the probability of its intrinsic growth rate being positive (assuming that positive and negative values are equally possible). Thus, the more $\omega(\boldsymbol{A})$ departs from the benchmark of 0.5, the larger the relevance of a nontrivial interaction matrix $\boldsymbol{A}$ to the feasibility of species.

5. Changes of species interactions and feasibility

In line with the majority of feasibility studies, so far we have assumed that species interactions do not change, i.e., there is only one interaction matrix $\boldsymbol{A}$. Yet, ecological communities are dynamic and permanently changing (Grant and Grant, 2014; Saavedra et al., 2016a; 2016b). Thus, the challenge is to integrate the information given by changes of species interactions under a systematic analysis of the feasibility domain (Cenci et al., 2018; Saavedra et al., 2017a). For instance, consider the case of a community that switches between two patterns of interactions characterized by the interaction matrices $\boldsymbol{A}$ and $\boldsymbol{B}$. Then, one can estimate the combined $\Omega(\boldsymbol{A}\cup\boldsymbol{B})$ or shared $\Omega(\boldsymbol{A}\cap\boldsymbol{B})$ normalized solid angles, i.e., the range of conditions for which the community is feasible by switching back and forth or under both matrices simultaneously. For this purpose, we can compute the union and the intersection of the feasibility domains of the matrices $\boldsymbol{A}$ and $\boldsymbol{B}$. Following the geometric representation of the feasibility domain, these can be written as:

$$\underbrace{\Omega(\boldsymbol{A}\cup\boldsymbol{B})}_{\text{combined feasibility}} = \Omega(\boldsymbol{A}) + \Omega(\boldsymbol{B}) - \underbrace{\Omega(\boldsymbol{A}\cap\boldsymbol{B})}_{\text{shared feasibility}}, \tag{7}$$

where $\Omega(\boldsymbol{A}\cup\boldsymbol{B}) = \mathrm{vol}((D_F(\boldsymbol{A})\cup D_F(\boldsymbol{B}))\cap\mathbb{B}^S)/\mathrm{vol}(\mathbb{B}^S)$ and $\Omega(\boldsymbol{A}\cap\boldsymbol{B}) = \mathrm{vol}((D_F(\boldsymbol{A})\cap D_F(\boldsymbol{B}))\cap\mathbb{B}^S)/\mathrm{vol}(\mathbb{B}^S)$.

The intersection of the two feasibility domains $D_F(\boldsymbol{A})$ and $D_F(\boldsymbol{B})$ can be algebraically formalized as the linear combination $\sum N_i^*\boldsymbol{v}_i$ of the spanning vectors of $\boldsymbol{A}$, where N_i^* satisfies

$$\begin{cases} \sum_{i=1}^{S} N_i^*\boldsymbol{v}_i = \sum_{i=1}^{S} \mu_i \boldsymbol{w}_i \\ N_i^*, \mu_i \geq 0, i = 1, \ldots, S, \end{cases} \tag{8}$$

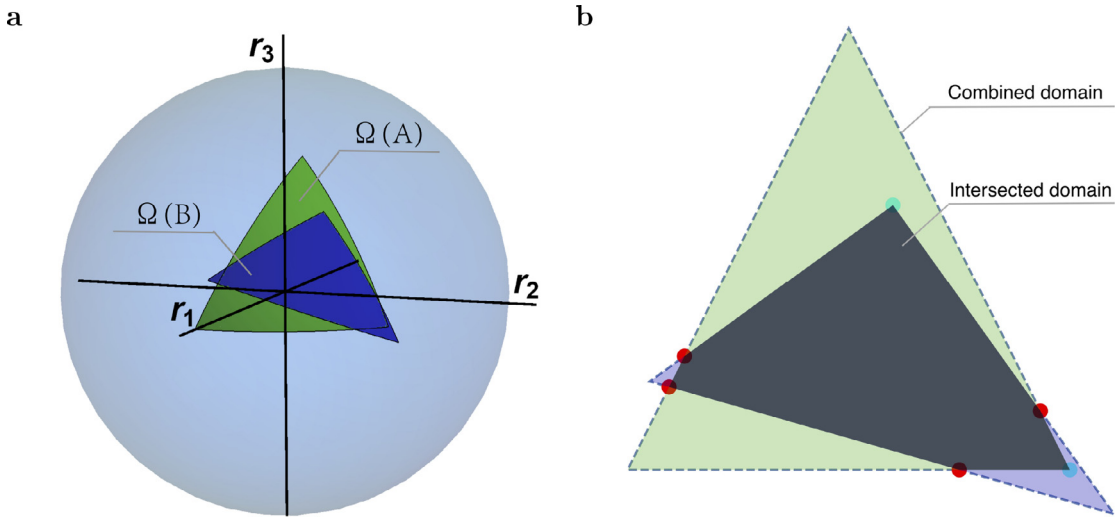

Fig. 2. Visualization of the combined and shared normalized solid angles generated by two feasibility cones. Panel **a** shows the combined space generated by two feasibility cones ($D_F(\boldsymbol{A})$ and $D_F(\boldsymbol{B})$) representing two different interaction matrices $\boldsymbol{A}$ and $\boldsymbol{B}$ formed by a fictitious community of three species. Panel **b** shows the geometric projection of the two feasibility cones. The combined, normalized, solid angle (area described by the dashed lines) is computed by the sum of the two relative volumes generated by the feasibility cones minus the relative volume generated by the intersection (overlap) between the cones. This intersection is shown by the dark region. Since the intersection of two polyhedrons can be triangulated (Hatcher, 2002), to find the overlap between the cones we have to locate the extreme points that generated the intersection. These are of two types: one type belongs to the original extreme points of each polyhedron (blue points), the other type belongs to the intersection of the edges of two polyhedrons (red points). See Appendix D for further details. (For interpretation of the references to color in this figure legend, the reader is referred to the web version of this article.)

and $\boldsymbol{v}_1, \ldots, \boldsymbol{v}_S$ and $\boldsymbol{w}_1, \ldots, \boldsymbol{w}_S$ are the spanning vectors of the cones $D_F(\boldsymbol{A})$ and $D_F(\boldsymbol{B})$, respectively (see Eq. (3)). Then, we need to apply the triangulation of the intersected region into several cones so that the intersected volume can be computed by adding the volume of each cone together through Eq. (6). See Fig. 2 for an illustration of this triangulation. The proof of the computational method and the code in R to compute $\Omega(\boldsymbol{A} \cap \boldsymbol{B})$ and $\Omega(\boldsymbol{A} \cup \boldsymbol{B})$ is archived on GitHub. As before, we can translate both the combined and the shared normalized solid angles from the community to the species level by defining $\omega(\boldsymbol{A} \cup \boldsymbol{B}) = \Omega(\boldsymbol{A} \cup \boldsymbol{B})^{1/S}$ and $\omega(\boldsymbol{A} \cap \boldsymbol{B}) = \Omega(\boldsymbol{A} \cap \boldsymbol{B})^{1/S}$, respectively.

6. Constraints on trophic energy flows and feasibility

Similarly, in line with the majority of feasibility studies, so far we have assumed that there are no constraints acting on energy flows across trophic levels modulating the values that the intrinsic growth rates can possibly take. Although this is a valid mathematical approach, these assumptions make little biological sense for many multi-trophic communities (Svirezhev and Logofet, 1983). In fact, numerous works have already introduced constraints on trophic energy flows in population dynamics models (Borrvall et al., 2000; Otto et al., 2007; Rossberg, 2013; Yodzis and Innes, 1992). For example, constraints on trophic energy flows in a food web can be translated into positive and negative intrinsic growth rates for basal and higher trophic levels, respectively (Rossberg, 2013)—i.e., a plant takes energy from the sun, but a lion cannot survive without prey. In this section, we will explain how to systematically incorporate these constraints into the study of feasibility. While our focus is on linear constraints, our methods can also be expanded to nonlinear constraints (see Appendix E).

In general, the effect of constraints can be formalized by:

$$\Omega_c(\boldsymbol{A} \cap \text{Constraints}) = \frac{\text{vol}(D_F(\boldsymbol{A}) \cap \text{Constraints} \cap \mathbb{B}^S)}{\text{vol}(\mathbb{B}^S \cap \text{Constraints})}. \tag{9}$$

This general definition implies that constraints can either increase or decrease the size of the feasibility domain of a community, depending on how the constraints intersect the feasibility domain of the interaction matrix and the closed unit ball. Note that constraints decrease both the volume in the numerator and that in the denominator; however, the decrease can be larger either in the numerator or denominator. Focusing on linear constraints, here we study linear inequalities and linear equalities (Bertsimas and Tsitsiklis, 1997). Linear inequalities allow us to take into account, for example, the sign constraints of intrinsic growth rates of species in the computation of the feasibility domain for a multi-trophic community. Linear equalities can allow us to incorporate, for example, as a first-order approximation, the correlations among intrinsic growth rates, such that species with similar constraints (or metabolic rates) could be constrained to have similar values (i.e., allometric relationships).

Formally, the most simple kind of linear inequalities in the intrinsic growth rates of a species i can be written as

$$L_i \leq r_i \leq U_i, \tag{10}$$

where L_i and U_i are the lower and upper bounds, respectively. Note that L_i and U_i do not depend on the intrinsic growth rates, nor on the properties of other species. They only depend on species i. Ecologically, this means that the intrinsic growth rates of some species are bounded. Importantly, these local constraints on individual species can introduce global constraints on the abundances of all species. Formally, we can write the constraints on the equilibrium species abundances $\boldsymbol{N}^*$ based on Eqs. (2) and (10) in the form of

$$L_i \leq \sum_{j=1}^{S} a_{ij} N_j^* \leq U_i \quad i = 1, \ldots, S, \tag{11}$$

where a_{ij} are the elements of the interaction matrix $\boldsymbol{A}$. These constraints shrink the feasibility cone to a bounded polytope of a convex subset of the original cone (Ball, 1997). See Fig. 3 for a graphical illustration.

Similarly, linear equalities can be formally introduced by assuming that two species i and j have exactly the same intrinsic growth rate. This constraint can be written explicitly as

$$\sum_{m=1}^{S} a_{im} N_m^* = \sum_{m=1}^{S} a_{jm} N_m^*. \tag{12}$$

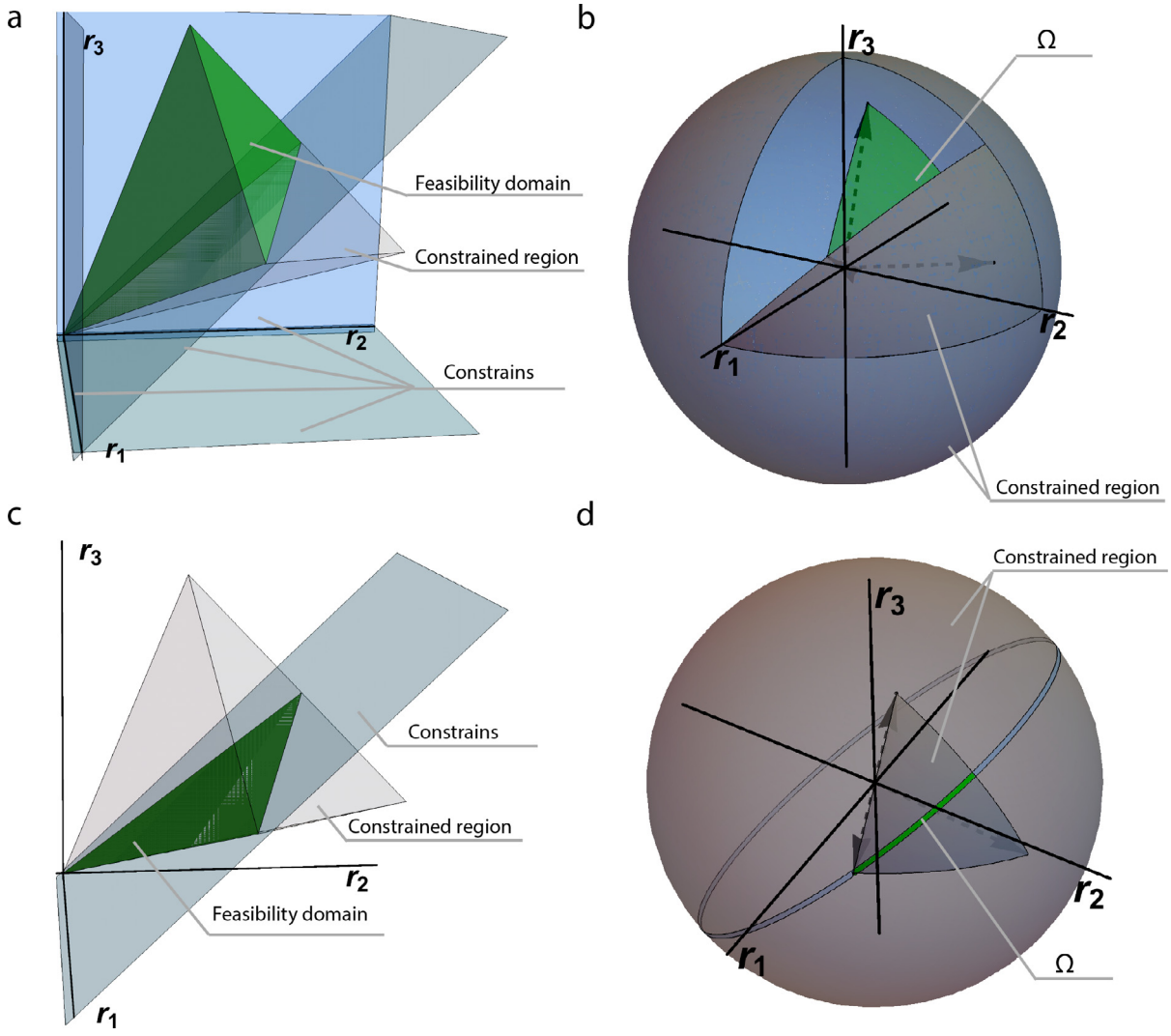

Fig. 3. Visualization of the feasibility domain with constraints imposed on energy flows across trophic levels. For a fictitious community of three species, the figures correspond to the parameter space of intrinsic growth rates ($\boldsymbol{r} = [r_1, r_2, r_3]^{\mathrm{T}}$). The green cones represent the feasibility cones generated by the column vectors of the interaction matrix negation ($-\boldsymbol{A}$) with linear constraints on intrinsic growth rates. Panel **a** shows the linear inequalities $r_3 \geq r_2$, and r_1, r_2, $r_3 \geq 0$ (represented by the gray area), which shrinks the feasibility cone and unit sphere. Panel **b** shows the constrained, normalized, solid angle that this constrained feasibility cone generates. Panel **c** shows the linear equality $r_2 = r_3$ on the feasibility cone (represented by the gray area), which projects the 3-dimensional cone into a 2-dimensional one. Similarly, Panel **d** shows the constrained, normalized, solid angle that this constrained feasibility cone generates.

A direct consequence of this constraint is that the dimension of the sampling space is reduced by one dimension. See Fig. 3 for a graphical illustration.

Linear constraints are strongly connected to linear programming (Bertsimas and Tsitsiklis, 1997), which can be integrated into the calculation of the constrained, normalized, solid angle $\Omega_c(\boldsymbol{A})$. Note that both the feasibility cone and the entire parameter space are reduced to the region of intrinsic growth rates dictated by the given linear constraints (see Fig. 3 for a graphical illustration). The code in R to introduce different linear constraints and compute $\Omega_c(\boldsymbol{A})$ is archived on GitHub. Note that there exists a close analytic formula to compute the expectation of $\Omega_c(\boldsymbol{A})$ for i.i.d. random matrices with constraints imposed on the abundances of species (Grilli et al., 2017). Similarly, the constrained, normalized, solid angle can be better represented by the constrained probability of feasibility of a species: $\omega_c(\boldsymbol{A}) = \Omega_c(\boldsymbol{A})^{1/S}$.

7. Illustrative example

To illustrate the application of our quantitative tools, we calculated the simple $\omega(\boldsymbol{A})$, combined $\omega(\boldsymbol{A} \cup \boldsymbol{B})$, shared $\omega(\boldsymbol{A} \cap \boldsymbol{B})$, and constrained $\omega_c(\boldsymbol{A})$ normalized solid angles at the species level of a simple 3-level trophic chain characterized by one basal, one consumer, and one top-predator species (see Fig. 4 for a graphical illustration). The elements a_{ij} of $\boldsymbol{A}$ for this trophic chain were randomly drawn from a normal distribution $N(0, 1)$, but the signs of the interactions were established according to the expected intake of food or energy (predator–prey interactions shown in Fig. 4). All species were assumed to be self-regulated (i.e., $a_{ii} = -1$). To calculate the combined and shared, normalized, solid angles of a hypothetical change of species interactions, we introduced small proportional random perturbations to the original matrix $\boldsymbol{A}$. These changes generated the new matrix $\boldsymbol{B}$. To calculate the constrained, normalized, solid angle we introduced sign constraints to the intrinsic growth rates of the basal (allowing only positive values) and predator species (allowing only negative values), following trophic energy constraints (Logofet, 1993; Rossberg, 2013). Fig. 4 summarizes the results of our example. Overall, the figure clearly shows that the relative size of the feasibility domain of ecological communities can significantly change depending on the biological information taken into consideration.

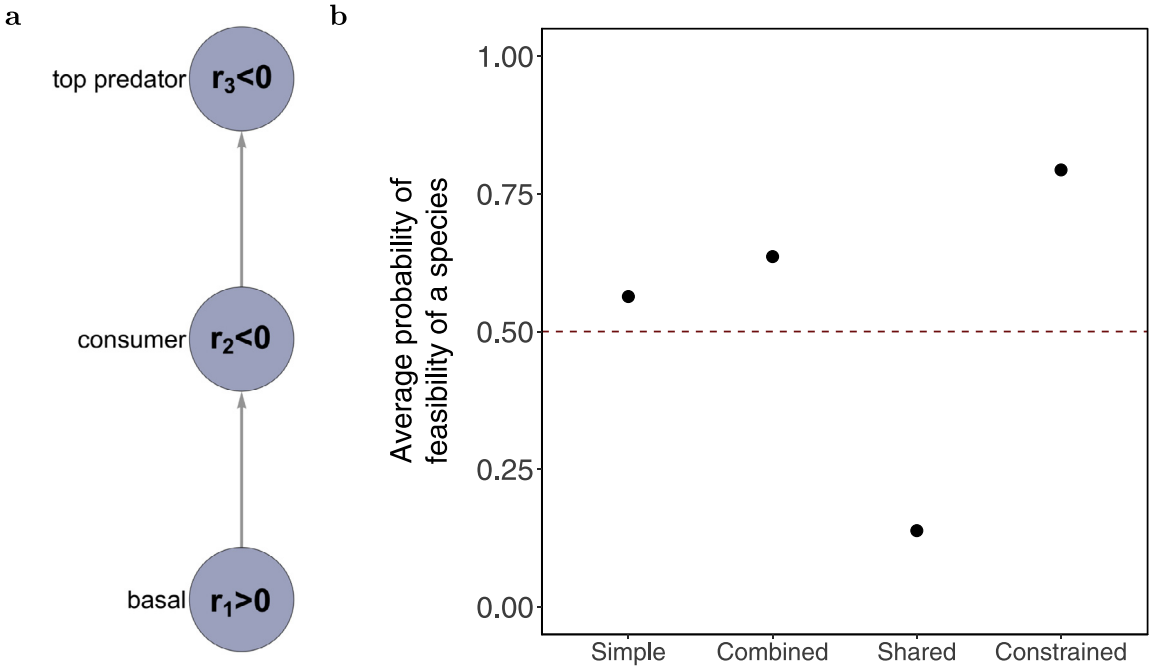

Fig. 4. Illustrative example of how the size of the feasibility domain changes as a function of adding biological information. The figure shows the simple $\omega(\boldsymbol{A})$, combined $\omega(\boldsymbol{A}\cup\boldsymbol{B})$, shared $\omega(\boldsymbol{A}\cap\boldsymbol{B})$, and constrained $\omega_c(\boldsymbol{A})$ normalized solid angles at the species level of a 3-level trophic community characterized by one basal, one consumer, and one top predator species. Panel **a** depicts a cartoon of this trophic chain. Each blue symbol corresponds to a species, whose intrinsic growth rate (shown inside the symbol) is constrained according to its position in the trophic chain. These species are linked by arrows showing the standard energy flow in the trophic chain. Panel **b** shows the different average probabilities of feasibility for a randomly chosen species in the trophic chain (normalized solid angles) that can be computed based on the biological information taken into account. See text for details on how the matrix, interaction changes, and constraints are generated. (For interpretation of the references to color in this figure legend, the reader is referred to the web version of this article.)

8. Conclusions

In this article, we have provided a basic quantitative guideline to help carry out a systematic analysis of the size of the feasibility domain for multi-trophic and changing ecological communities. While numerous and important work has been devoted to the analysis of feasible communities, there is still a central and urgent gap to fill regarding how to integrate feasibility analysis with additional biological information into a rigorous methodological framework. Typically, the majority of work on feasibility assumed either no structure of species interactions, a static view of communities, or that energy flows can happen equally across trophic levels. However, this may violate central biological principles depending on the developmental stage of a community (Odum, 1969). Thus, it becomes essential to have tools that can allow us to explore the extent to which all of this information is necessary for a better understanding about the conditions leading to feasible ecological communities, and the limits at which communities may no longer tolerate environmental perturbations (Cenci et al., 2017). In this direction, our tools have shown that, by integrating these biological properties, the size of the feasibility domain of ecological communities can drastically change. Moreover, constraints on trophic energy flows can significantly increase the feasibility domain, which may provide a potential explanation for the prevalence of such configurations. Yet, more work on this area needs to be done before reaching any final conclusions.

As potential new directions derived from our guideline, first we would like to stress how important is the probabilistic interpretation of our measures. Since communities are permanently changing and it is extremely difficult to field parameterize a population dynamics model involving more than 2 species (Vandermeer, 1975), the concept of how likely different parameterizations lead to a feasible community can be mapped back onto how likely a community of species can coexist under given and changing environmental conditions. Of course, feasibility is only a necessary, but not a sufficient condition for species coexistence (Hofbauer and Sigmund, 1998), which implies that other dynamical properties that could grant this sufficiency when found along with feasibility (such as dynamical stability) should be explored under a similar framework (Arnoldi and Haegeman, 2016; Song and Saavedra, 2018). We also believe that species-based metrics of feasibility, such as the rescaled volume of the feasible domain $\omega(\boldsymbol{A})$, can provide a more intuitive interpretation of the community feasibility, especially when comparing communities of different dimensions.

In particular, we encourage the investigation of potential trade-offs involved during changes in species interactions by moving communities from unfeasible to feasible regions and vice versa. For instance, as we have seen in Fig. 4, changes of species interactions can increase the feasibility of a community, as expressed by the combined feasibility between interaction matrices $\boldsymbol{A}$ and $\boldsymbol{B}$. However, these changes could require a very different set of intrinsic growth rates to which species might even not be able to adapt. This can be captured by the fraction $\omega(\boldsymbol{A}\cap\boldsymbol{B})/\omega(\boldsymbol{A})$, where the higher the value, the larger the range of intrinsic growth rates shared between the feasibility cones $D_F(\boldsymbol{A})$ and $D_F(\boldsymbol{B})$. Thus, it might not always be possible for a community to increase both its combined and shared, normalized, solid angles at the same time, suggesting a trade-off between feasibility and adaptability. Future studies could investigate this type of trade-offs during the development and reorganization of ecological communities.

Similarly, introducing constraints on trophic energy flows can help us to infer parameterizations, to identify missing or improbable interspecific interactions, or to study the effect of parameter correlations on the feasibility of ecological communities. Moreover, these constraints can help us to shift the focus from the structure of species interactions to the structure of the parameter space, which appears to be a necessary step towards a better understanding of species persistence (Saavedra et al., 2017b). Overall, we envi-

sion that tools like the ones presented in this guideline can open a new and prosperous dialogue for a stronger synthesis of theoretical and empirical work on multi-trophic and changing communities.

Competing financial interests The authors declare no competing financial interests.

Author contributions All authors designed the study. CS derived proofs, wrote the computational code, and performed the study. SS supervised the study and wrote a first version of the manuscript. All authors contributed with significant revisions to the manuscript.

Data accessibility Should the manuscript be accepted, The code in R supporting the results is archived in Github: https://github.com/clsong/JTB-Song_et_al-2018.

Acknowledgment

We would also like to thank two anonymous referees for their highly constructive comments that helped us to improve our manuscript. Funding was provided by the MIT Research Committee Funds and the Mitsui Chair.

Supplementary material

Supplementary material associated with this article can be found, in the online version, at doi:10.1016/j.jtbi.2018.04.030.

References

Arnoldi, J.-F., Haegeman, B., 2016. Unifying dynamical and structural stability of equilibria. Proc. R. Soc. Lond. A 472, 20150874.
Ball, K., 1997. An elementary introduction to modern convex geometry. Flavors Geometry 31, 1–58.
Bastolla, U., Fortuna, M.A., Pascual-García, A., Ferrera, A., Luque, B., Bascompte, J., 2009. The architecture of mutualistic networks minimizes competition and increases biodiversity. Nature 458, 1018–1020.
Bertsimas, D., Tsitsiklis, J.N., 1997. Introduction to Linear Optimization, 6. Athena Scientific, Belmont.
Borrvall, C., Ebenman, B., Jonsson, T., 2000. Biodiversity lessens the risk of cascading extinction in model food webs. Ecol. Lett. 2, 131–136.
Brondsted, A., 2012. An Introduction to Convex Polytopes, 90. Springer Science & Business Media, Medford.
Bruneau, L., Germinet, F., 2009. On the singularity of random matrices with independent entries. Proc. Am. Math. Soc. 137, 787–792.
Case, T.J., 2000. An Illustrated Guide to Theoretical Ecology. Oxford University Press, Oxford.
Cenci, S., Montero-Castaño, A., Saavedra, S., 2018. Estimating the effect of the reorganization of interactions on the adaptability of species to changing environments. J. Theor. Biol. 437, 115–125.
Cenci, S., Saavedra, S., 2018. Structural stability of nonlinear population dynamics. Phys. Rev. E 97, 012401.
Cenci, S., Song, C., Saavedra, S., 2017. Rethinking the importance of the structure of ecological networks under an environment-dependent framework. BioRxiv doi:10.1101/219691.
Coulson, T., Kendall, B.E., Barthold, J., Plard, F., Schindler, S., Ozgul, A., Gaillard, J.M., 2017. Modeling adaptive and nonadaptive responses of populations to environmental change. Am. Nat. 190, 313–336.
Genz, A., Bretz, F., 2002. Comparison of methods for the computation of multivariate t probabilities. J. Comput. Graph. Stat. 11, 950–971.
Gilpin, M.E., 1975. Stability of feasible predator-prey systems. Nature 254, 137–139.
Goh, B., Jennings, L., 1977. Feasibility and stability in randomly assembled Lotka–Volterra models. Ecol. Modell. 3, 63–71.
Gourion, D., Seeger, A., 2010. Deterministic and stochastic methods for computing volumetric moduli of convex cones. Comput. Appl. Math. 29, 215–246.
Grant, P.R., Grant, B.R., 2014. 40 Years of Evolution. Darwinâ;;s Finches on Daphne Major Island. Princeton University Press, Princeton.
Grilli, J., Adorisio, M., Suweis, S., Barabás, G., Banavar, J.R., Allesina, S., Maritan, A., 2017. Feasibility and coexistence of large ecological communities. Nat. Comm. 8, 14389.
Hatcher, A., 2002. Algebraic Topology. Cambridge University Press, Cambridge.
Hofbauer, J., Sigmund, K., 1998. Evolutionary Pames and Population Dynamics. Cambridge University Press, Cambridge.
Levins, R., 1968. Evolution in Changing Environments: Some Theoretical Explorations. Princeton University Press, NJ.
Logofet, D.O., 1993. Matrices and graphs. Stab. Prob. Math. Ecol.. CRC, Boca Ratón, FL
MacArthur, R., 1970. Species packing and competitive equilibrium for many species. Theor. Popul. Biol. 1, 1–11.
Meszéna, G., Gyllenberg, M., Pásztor, L., Metz, J.A.J., 2006. Competitive exclusion and limiting similarity: a unified theory. Theor. Popul. Biol. 69, 68–87.
Odum, E.P., 1969. The strategy of ecosystem development. Science 164, 262–270.
Otto, S.B., Rall, B.C., Brose, U., 2007. Allometric degree distributions facilitate food-web stability. Nature 450, 1126–1229.
Page, K.M., Nowak, M.A., 2002. Unifying evolutionary dynamics. J. Theor. Biol. 219, 93–98.
Pimm, S.L., 1982. Food webs. Food Webs. Springer, Medford.
R Core Team, 2017. R: A Language and Environment for Statistical Computing. R Foundation for Statistical Computing, Vienna, Austria. https://www.R-project.org/.
Ribando, J.M., 2006. Measuring solid angles beyond dimension three. Discrete Comput. Geometry 36, 479–487.
Roberts, A., 1974. The stability of a feasible random ecosystem. Nature 251, 607–608.
Rohr, R.P., Saavedra, S., Bascompte, J., 2014. On the structural stability of mutualistic systems. Science 345, 1253497.
Rohr, R.P., Saavedra, S., Peralta, G., Frost, C.M., Bersier, L.-F., Bascompte, J., Tylianakis, J.M., 2016. Persist or produce: a community trade-off tuned by species evenness. Am. Nat. 188, 411–422.
Rossberg, A.G., 2013. Food Webs and Biodiversity. Wiley, Hoboken.
Roughgarden, J., 1975. A simple model for population dynamics in stochastic environments. Am. Nat. 109, 713–736.
Saavedra, S., Cenci, S., del Val, E., Boege, K., Rohr, R.P., 2017a. Reorganization of interaction networks modulates the persistence of species in late successional stages. J. Anim. Ecol. 86, 1136–1146.
Saavedra, S., Rohr, R.P., Bascompte, J., Godoy, O., Kraft, N.J.B., Levine, J.M., 2017b. A structural approach for understanding multispecies coexistence. Ecol. Monogr. 87, 470–486.
Saavedra, S., Rohr, R.P., Fortuna, M.A., Selva, N., Bascompte, J., 2016a. Seasonal species interactions minimize the impact of species turnover on the likelihood of community persistence. Ecology 97, 865–873.
Saavedra, S., Rohr, R.P., Gilarranz, L.J., Bascompte, J., 2014. How structurally stable are global socioeconomic systems? J. R. Soc. Interface 11.
Saavedra, S., Rohr, R.P., Olesen, J.M., Bascompte, J., 2016b. Nested species interactions promote feasibility over stability during the assembly of a pollinator community. Ecol. Evol. 6, 997–1007.
Song, C., Saavedra, S., 2018. Will a small randomly-assembled community be feasible and stable. Ecology 99, 743–751.
Stone, L., 2016. The google matrix controls the stability of structured ecological and biological networks. Nat. Comm. 7, 12857.
Sugihara, G., May, R., Ye, H., Hsieh, C.-h., Deyle, E., Fogarty, M., Munch, S., 2012. Detecting causality in complex ecosystems. Science 338, 496–500.
Svirezhev, Y.M., Logofet, D.O., 1983. Ustoichivost biologicheskih soobschestv (1978) Nauka, Moscow (in Russian). English translation: Stability of biological communities. MIR Publishers, Moscow.
Takeuchi, Y., 1996. Global dynamical properties of Lotka-Volterra systems. World Scientific, Danvers.
Vandermeer, J.H., 1975. Interspecific competition: a new approach to the classical theory. Science 188, 253–255.
Yodzis, P., Innes, S., 1992. Body size and consumer-resource dynamics. Am. Nat. 139, 1151–1175.

Appendix

A guideline to study the feasibility domain of multi-trophic and changing ecological communities

Chuliang Song[1], Rudolf P. Rohr[2], Serguei Saavedra[1*]

[1]Department of Civil and Environmental Engineering, MIT
77 Massachusetts Av., 02139 Cambridge, MA, USA
[2]Department of Biology - Ecology and Evolution, University of Fribourg
Chemin du Musée 10, CH-1700 Fribourg, Switzerland.

A Definition of feasibility domain

Here, we briefly present the formal definitions associated with the feasibility domain.

Definition 1 (Feasibility Domain)**.** *The feasibility domain for a non-singular interaction matrix* $\mathbf{A}$ *is defined as the parameter space of intrinsic growth rates that leads to a feasible (positive) equilibrium, i.e., the set of* $\mathbf{r}$ *such that* $-\mathbf{A}^{-1}\mathbf{r} > 0$*.*

Definition 2 (Cone)**.** *A cone in* $\mathbb{R}^S$ *is defined as a space spanned by positive linear combinations of* S *linearly independent vectors.*

Remark 1. *This is also referred as a simplicial cone (Ribando, 2006). For simplicity, we will call it cone. However, it is important to note that this is not the common definition of cone (James, 1992).*

Definition 3 (Spanning Vector)**.** *The vector* $\mathbf{v}_i$ *is defined as the* i^{th} *spanning vector of the feasibility domain if* $\mathbf{v}_i$ *is the negation of the* i^{th} *column of* $\mathbf{A}$*.*

Remark 2. *A spanning vector is sometimes referred to as an extreme ray in convex geometry (Bertsimas & Tsitsiklis, 1997).*

With the above definitions, the feasibility domain of $\mathbf{A}$ is proved to be (Svirezhev & Logofet, 1983)

$$D_F(\boldsymbol{A}) = \{\boldsymbol{r} = N_1^*\boldsymbol{v}_1 + \cdots + N_S^*\boldsymbol{v}_S, \text{ with } N_1^* > 0, \ldots, N_n^* > 0\}\,, \tag{A1}$$

where $\mathbf{v}_i$ is the negation of the i^{th} column of $\mathbf{A}$.

Remark 3. *This definition is the reason why we restrict the parameters, in the definition of cone, to be strictly greater than* 0*, instead of the standard definition where the boundary is also included.*

Remark 4. *The non-singularity condition* $\mathsf{det}(\mathbf{A}) \neq 0$ *is equivalent to the situations where* $(\mathbf{v}_1, ..., \mathbf{v}_S)$ *are linearly independent. The non-singular interaction matrix* $\mathbf{A}$ *gives a one-to-one linear mapping from the feasibility domain to the space of positive equilibrium of species abundances. Mathematically, these two spaces are equivalent. However, the geometric representation and the clear link to the interaction matrix makes this transformation useful for feasibility analysis (Saavedra et al., 2017b).*

B Least upper bound of the relative volume

Here, we prove a basic property of the normalized solid angle $\Omega(\mathbf{A})$ (defined in eqn. 5).

Theorem 1. *Least upper bound of* $\Omega(\mathbf{A})$ *is* $\frac{1}{2}$.

Proof. First we prove that $\frac{1}{2}$ is an upper bound for $\Omega(\mathbf{A})$, then we prove that this upper bound is a limit point.

The relative volume is generated by the positive linear combinations of S linearly independent vectors $\mathbf{v}_1, ..., \mathbf{v}_S$. The end-points of those vectors form a hyperplane that does not pass through the origin because of the assumption of linear independence. Let us consider the hyperplane that passes through the origin and is parallel to the hyperplane formed by the end-points of our S vectors. By construction, all the end-points are on the same side of the hyperplane. Because the normalized solid angle of the whole side of a hyperplane is $\frac{1}{2}$, it is proved that $\frac{1}{2}$ is an upper bound of $\Omega(\mathbf{A})$.

Then we prove that $\frac{1}{2}$ is a limit point. Let us construct the following set of S vectors:

$$\mathbf{v}_1 = \begin{pmatrix} 1 \\ 0 \\ \vdots \\ 0 \end{pmatrix}, \mathbf{v}_2 = \begin{pmatrix} 0 \\ 1 \\ \vdots \\ 0 \end{pmatrix}, \cdots, \text{ and } \mathbf{v}_S = \begin{pmatrix} -1 \\ -1 \\ \vdots \\ \delta \end{pmatrix}.$$

For $\delta > 0$, those S vectors are linearly independent and generate a cone of a normalized solid angle $\Omega(\mathbf{A}) < \frac{1}{2}$. By taking the limit$\delta \to 0^+$, the normalized solid angle $\Omega(\mathbf{A}) \to \frac{1}{2}$. This proves that $\frac{1}{2}$ is a least upper bound of $\Omega(\mathbf{A})$.

□

C Computation of the relative volume

Here, we discuss the computation of the normalized solid angle $\Omega(\mathbf{A})$. In the main text (Eqn. (6)), we have presented an analytic formula. In fact, Ribando (2006) proved a closed form to compute the normalized solid angle $\Omega(A)$ (Theorem 2.2. in (Ribando, 2006)). However, this formula is computationally expensive in high dimension, and an exact solution is not actually needed. Thus, we use a quasi-Monte Carlo method to efficiently compute the relative volume following Genz & Bretz (2002); Saavedra et al. (2016b). One important computational consideration is the numerical error of $(\mathbf{A}^T\mathbf{A})^{-1}$, which is a quantity required for the computation of the normalized solid angle. For instance, the tolerance level of the function *solve* in R is too low for high dimensions. In order to correct for these numerical errors, we encourage to use the function *chol2inv* in R, or any other function incorporating the QR decomposition to compute the inverse of the matrix (Trefethen & Bau III, 1997).

D Intersection of feasibility cones

Here, we turn our attention to the overlap (intersection) of two (or more) feasibility cones corresponding to two (or more) interaction matrices of the same dimension. Without loss of generality, we will focus on two cones. To calculate this overlap, one can think about the problem of computing the probability of the intersection of two events U_1 and U_2, namely $\Omega(U_1 \cap U_2)$. This intersection is needed to calculate the combined $\Omega(\mathbf{A} \cup \mathbf{B})$ and shared $\Omega(\mathbf{A} \cap \mathbf{B})$ normalized solid angles between two (or more) feasibility cones $D_F(\mathbf{A})$ and $D_F(\mathbf{B})$ (see main text): $\Omega(\mathbf{A} \cup \mathbf{B}) = \Omega(\mathbf{A}) + \Omega(\mathbf{B}) - \Omega(\mathbf{A} \cap \mathbf{B})$.

The overlap of two feasibility cones is not a trivial problem in computation. However, using convex geometry, we can translate the overlap problem into an *affine space* of the cones problem (Leichtweiß, 1999). That is, we can take the advantage of the fundamental fact that any spanning vector starting from the origin is uniquely determined by any point on it except for its initial point. Importantly, this guarantees that any feasibility cone can be compressed without loss of information into its intersection with a hyperplane (polyhedron), which can be chosen arbitrarily as long as the intersection is not empty.

Therefore, we can study the geometric properties corresponding to the overlap between two S-dimensional cones simply by choosing a hyperplane that intersects both feasibility cones when the overlap is nonempty, and then investigate the overlap of two polyhedrons on the $(S-1)$-dimensional hyperplane. Because the intersection of two polyhedrons can be triangulated (Hatcher, 2002), all we have to do (if the overlap is a non-empty set) is to locate the extreme points that generated the intersection. This is the key observation that simplifies the computation of the overlap between two feasibility cones. That is, the intersection is generated by two types of points: one type belongs to the original extreme points of each polyhedron, and the other type belongs to the intersection of the edges of two polyhedrons. Note that the affine transformation only preserves the relative position rather than the relative volume of a geometric object (Kostrikin, 1982), the volume of intersection cannot be simply calculated as the absolute volume of the intersection over the volume of the two polyhedrons on the hyperplane. Below, we provide the full derivation.

The overlap is mathematically defined as Eqn. (8) in the main text. It may not be a cone, and the following theorem describes its shape.

Theorem 2. *The overlap of two feasibility cones is a union of cone(s), or an empty set.*

Proof. An empty overlap is obviously possible. We discuss the case when the overlap is not empty. Let us denote two feasibility cones as $D_F(\boldsymbol{A})$ and $D_F(\boldsymbol{B})$, respectively.

First, we prove that the overlap is a polyhedron with only extreme rays. Suppose $\sum_{i=1}^{S} a_i \mathbf{v}_i$ is inside the overlap, then for any positive $\lambda > 0$, $\lambda \sum_{i=1}^{S} a_i \mathbf{v}_i$ is inside the overlap, too. Also, the overlap of two cones is still a polyhedron. Thus, by the resolution theorem (Bertsimas & Tsitsiklis, 1997), there exist extreme rays $\mathbf{v}_1, .., \mathbf{v}_N$ such that the overlap is equivalent to

$$\{\sum_{i=1}^{N} \lambda_i \mathbf{v}_i | \lambda_1, ..., \lambda_N > 0\}. \tag{D1}$$

Second, we prove that $N = S$ if the borders of the two cones do not intersect. From the view of the parameter space, $D_F(\boldsymbol{A})$ separates the Euclidean space into three disjoint sets: $\mathscr{C}_1 = \{\lambda|\lambda_i < 0, \exists i\}$ (outside the cone), $\mathscr{C}_2 = \{\lambda|\lambda_i = 0, \exists i\}$ (the borders of the cone), $\mathscr{C}_3 = \{\lambda|\lambda_i > 0, \forall i\}$ (inside the cone). If the feasibility cone $D_F(\boldsymbol{B})$ intersects with both $\mathscr{C}_1$ and $\mathscr{C}_3$ of $D_F(\boldsymbol{A})$, then by continuity, $D_F(\boldsymbol{B})$ also intersects with $\mathscr{C}_2$ of $D_F(\boldsymbol{A})$. Since the overlap is assumed to be non-empty, $D_F(\boldsymbol{B})$ must be contained in either $\mathscr{C}_1$ or $\mathscr{C}_3$ of $D_F(\boldsymbol{A})$. In both cases, $N = S$.

Finally, we prove that $N \geq S$ if the borders of the two simplexes intersect. If $N < S$, then the overlap is null (Stein & Shakarchi, 2009). Since the borders intersect, the border of a cone is not in the cone. Then by the assumption of non-emptiness, there must exist one point x_0 inside the overlap. Because this point is in the interior of $D_F(\boldsymbol{A})$, there exists a $\epsilon_A > 0$ such that the neighborhood $\{x \mid |x - x_0| < \epsilon_A\}$ of x_0 is inside $D_F(\boldsymbol{A})$. Similarly, there exists an $\epsilon_B > 0$ such that the neighborhood $\{x \mid |x - x_0| < \epsilon_B\}$ of x_0 is inside $D_F(\boldsymbol{B})$. Thus, the neighborhood $\{x \mid |x - x_0| < min\{\epsilon_A, \epsilon_B\}\}$ of x_0 is in the overlap whose measure is nonzero, which leads to a contradiction. Thus, $N \geq S$ if the overlap is not empty. The set of N vectors can be $\cup U_i$, where the cardinality of each U_i is S, and any element in U_i is not in the interior of the polyhedron spanned by $U_j, \forall j \neq i$. This can easily be proved by mathematical induction. □

The problem left now is to compute the extreme rays. We reformulate it by transforming it into an equivalent problem.

Definition 4 (Characteristic Simplex of a Cone)**.** *A characteristic simplex of a cone is defined as the interior of the convex set whose extreme points are located on the spanning vectors. See Fig. D1 for an illustration.*

Corollary 1. *The characteristic simplex of a feasibility cone is an $(S-1)$-dimensional simplex.*

Proof. Let us denote the intersection points as $v_i,\ i = 1, ..., S$. Then, the simplex is equivalent to

$$\{\mathbf{r} = \sum_{i=1}^{S} \lambda_i \mathbf{v}_i \in \mathrm{R}^n | \exists \lambda_1, .., \lambda_S > 0, \sum_{i=1}^{S} \lambda_i = 1\}. \tag{D2}$$

Since we only consider non-degenerate cases, $\mathbf{v}_i$ are linearly independent. Thus, it satisfies the standard definition of a simplex. □

Remark 5. *The border is included in the standard definition of a simplex, while the definition of a characteristic simplex excludes the border.*

Definition 5 (Associated Polyhedron)**.** *The associated polyhedron of a feasibility cone is defined as the polyhedron whose extreme points are the origin point and the spanning vectors (taken as points). The associated face of the polyhedron corresponds to the face spanned by the spanning vectors of the original cone.*

Theorem 3. *The spanning vectors of the intersection of two feasibility cones are extreme points of the overlap of the corresponding characteristic simplexes.*

Proof. Let us denote the two feasibility cones as $D_F(\boldsymbol{A})$ and $D_F(\boldsymbol{B})$, and the interaction matrices as $\boldsymbol{A}, \boldsymbol{B}$. Also, denote the intersection with the associated face of $\boldsymbol{A}$ as F_A, and with $\boldsymbol{B}$ as F_B.

The overlap of $D_F(\boldsymbol{A})$ and $D_F(\boldsymbol{B})$ can be written as

$$\{\mathbf{r} | A^{-1}\mathbf{r}, B^{-1}\mathbf{r} \in (\mathbb{R}_-)^S\}. \tag{D3}$$

The overlap of F_A and F_B can be written as

$$\{\mathbf{r}|A^{-1}\mathbf{r}, B^{-1}\mathbf{r} \in (-1,0)^S\}. \tag{D4}$$

where $(-1,0)^S$ is the Cartesian product.
The intersection of the overlap and the associated face of any cone is equivalent to the overlap. By uniqueness of extreme points and extreme rays in convex geometry, the proof is complete. □

Remark 6. *By convex geometry, the overlap of F_A and F_B can be uniquely determined by its extreme points, and the overlap of $D_F(\boldsymbol{A})$ and $D_F(\boldsymbol{B})$ can be uniquely determined by its extreme rays (spanning vectors). Thus, this theorem proves the equivalence of these two definitions via construction.*

The vertexes of the simplex and the intersection points of simplexes are candidates as extreme points of the overlap.

Theorem 4. *The extreme points of the overlap of characteristic simplexes are the extreme points of the joint of the set of all vertexes of one simplex in another simplex's closure. This closure has the set of the intersection points of the edges of one simplex with borders of another simplex.*

Proof. We consider the closure of the overlap. This is only for mathematical simplicity due to the fact that an extreme point is equivalent to a basic feasible solution under this setup (Bertsimas & Tsitsiklis, 1997). All vertexes of the simplexes are basic solutions, thus, it is an extreme point if and only if it is feasible.

All extreme points must be in the intersection of the borders of the simplexes. Let us consider a face which has a subset that is in the border of the overlap. We show that any extreme point x_0 of the overlap that is in this face must be on some edge of another simplex. Otherwise, x_0 must be in the interior of some face F_2 of another simplex. Thus, F_A transverse F_B is restricted to the overlap part of F_1 and F_2 (Guillemin & Pollack, 2010), which in turn gives that x_0 is not in the border of the overlap part. See Fig. D2 for a visualization of this geometric idea. □

In general, to enumerate all vertexes of a polyhedron is difficult (Khachiyan et al., 2008). No algorithm in polynomial time has been found for solving the general case (Murty, 2009). For a particular case, the total number of vertexes might be exponential by the constraints. Due to the geometric essence of the problem, the maximum number of extreme points grows only squarely with the dimension.

Definition 6 (Notations)**.** *For a set of vectors $\mathbf{v}_1, ..., \mathbf{v}_N$, expression $(\mathbf{v}_1, .., \bar{\mathbf{v}}_i, ..., \mathbf{v}_N)$ denotes the space spanned by all vectors but $\mathbf{v}_i$. For a set $\mathscr{A}$, $\bar{\mathscr{A}}$ denotes the closure of $\mathscr{A}$, and $\mathscr{A}^{\mathrm{o}}$ denotes the interior of $\mathscr{A}$.*

Theorem 5. *The maximum number of the spanning vectors of the intersection of two feasibility cones is $S(S-1)$.*

Proof. We first prove that any edge of $D_F(\boldsymbol{A})$ will not intersect with more than interiors of two faces of $D_F(\boldsymbol{C})$. Suppose that an edge has passed three faces of $D_F(\boldsymbol{B})$. Without loss of generality, let us suppose the middle one is on the face spanned by $(\bar{\mathbf{v}}_1, .., \mathbf{v}_{S-1}, \mathbf{v}_S)$, and the other two are on the face spanned by $(\mathbf{v}_1, .., \mathbf{v}_{S-1}, \bar{\mathbf{v}}_S)$ and $(\mathbf{v}_1, .., \bar{\mathbf{v}}_{S-1}, v_S)$, respectively. Then, there exists $k_1, k_2 > 0$, such that

$$k_1\lambda_1 + k_2\lambda_2 = 0, \tag{D5}$$

where λ_1, λ_2 are the positive coefficients of $\mathbf{v}_1$ in the two border points. This is in fact not possible.

Thus, there are no more than $S-1$ extreme points on each face. In total, there can be no more than $2S(S-1)$ on all faces of two simplexes. If an extreme point is on the interior of some face, then it is counted at least twice; if an extreme point is on the interior of some edge, then it is counted at least $S-1$ times; if an extreme point is on some vertex, then it is counted at least S times. Thus, there can be no more than $S(S-1)$ different extreme points.

The positioning of the simplexes that gives the highest number of extreme points can be constructed: for each face of $D_F(\boldsymbol{A})$, there are $S-1$ vertexes of $D_F(\boldsymbol{B})$ on the side of the face where the vertex of $D_F(\boldsymbol{A})$ that does not belong to this face, and only one vertex of $D_F(\boldsymbol{B})$ on the other side. In this case, the number of extreme points is $(S-1)S$. Thus, the upper bound is tight. □

By theorem 2, 3, and 5, the non-empty overlap of the original feasibility cones has at most $S(S-1)$ spanning vectors and at least S spanning vectors. Now the problem is reduced to separate the overlap of cones into several disjoint cones.

Definition 7 (Border set)**.** *A subset of spanning vectors with S elements is defined as a border set if all spanning vectors that are not in this subset are on one side of the space spanned by this subset.*

Theorem 6. *Let us suppose a set of N vectors where any S elements are linearly independent. The problem is to partition this set into $\cup U_i$, where by cardinality of each U_i is S, and any element in U_i is not in the interior of the polyhedron spanned by $U_j, \forall j \neq i$. Each U_i is defined as a partitioning set. The computational complexity of this problem is in polynomial time.*

Proof. The simplexes referred following are characteristic simplexes. This approach is justified by theorem 3.

We first prove that the total number of these partitioning sets is $N - S + 1$. This is because each of the two cones whose corresponding characteristic simplexes share a face have S_1 spanning vectors in common. Note that two different characteristic simplexes cannot share two faces. This is because two faces involve all the spanning vectors, which uniquely determine a partitioning set. The characteristic simplex of any cone must share at least one face with another simplex. Note that the points in one border set must be on the same face of some simplex. See Fig. D3 for a visualization of this geometric idea. □

Following Ribando (2006) and Theorem 6, the problem of computing analytically the overlap is solved.

Remark 7. *Our results show that the overlap of two arbitrary cones can be analytically computed as there is a closed form (Ribando, 2006). Note that our results do not contradict the classical result: that computing the precise volume of the polyhedron in high dimension is an $\#P$-complete problem (Khachiyan, 1989; Dyer & Frieze, 1988).*

Clearly, the methodology above can be applied to the intersection of multiple feasibility cones. All the code in R will be archived on Github.

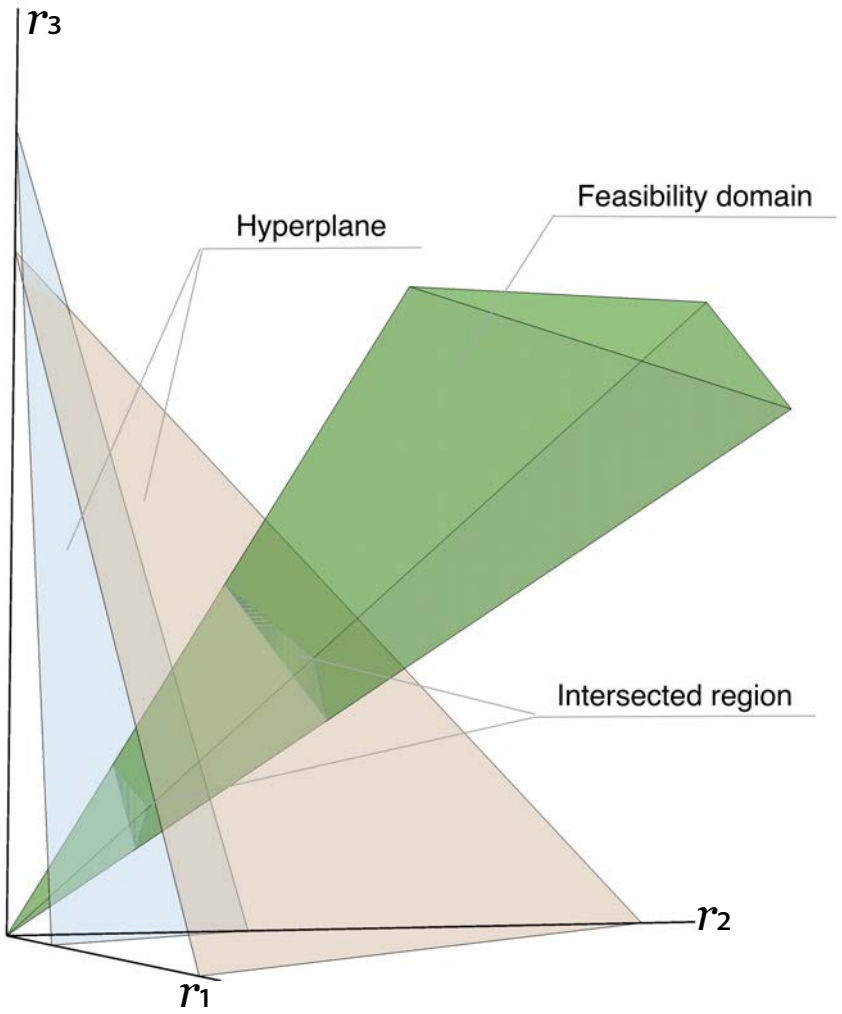

Figure D1: **Characteristic Cones**. The nonempty intersections of the feasibility cone with any hyperplane are equivalent up to affine transformation.

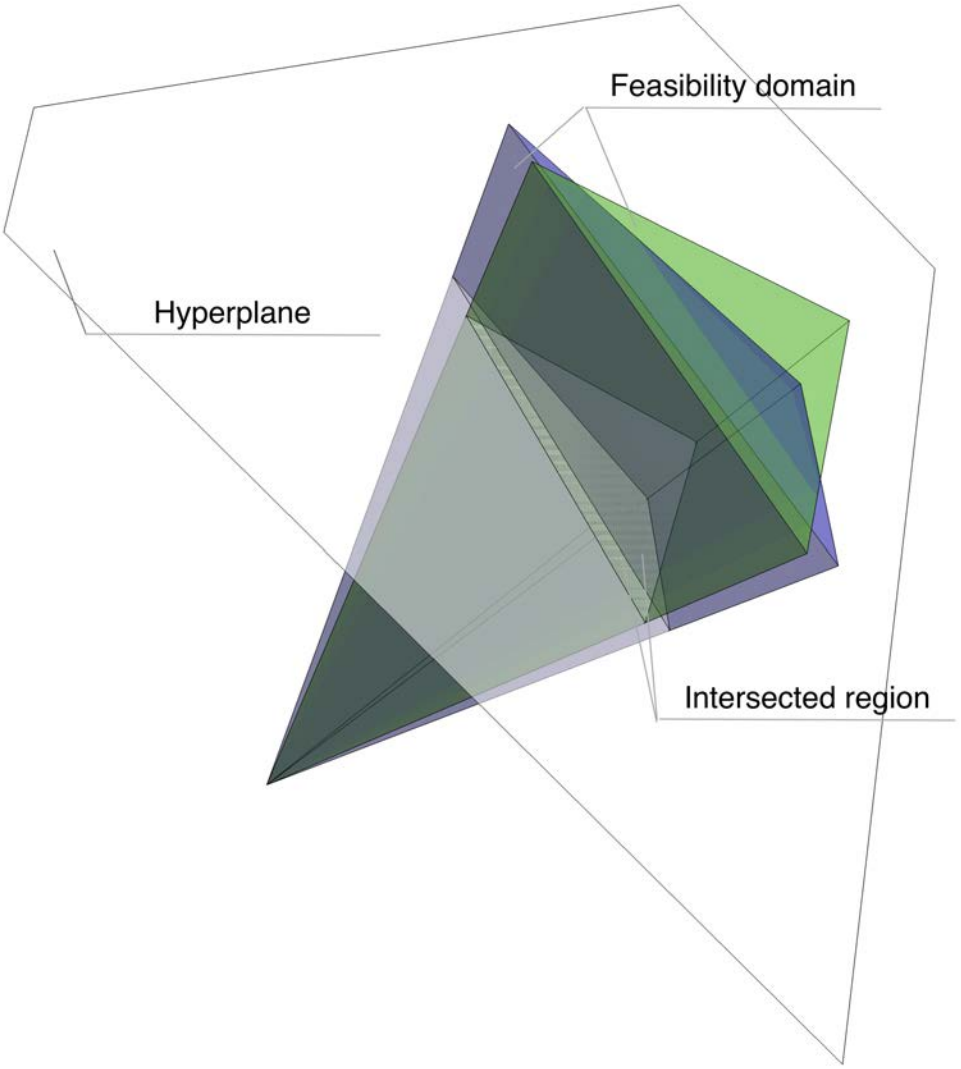

Figure D2: **Intersection of Cones**. This transforms the original problem into an equivalent question, the extreme points of the intersection of two $S-1$ closed simplex.

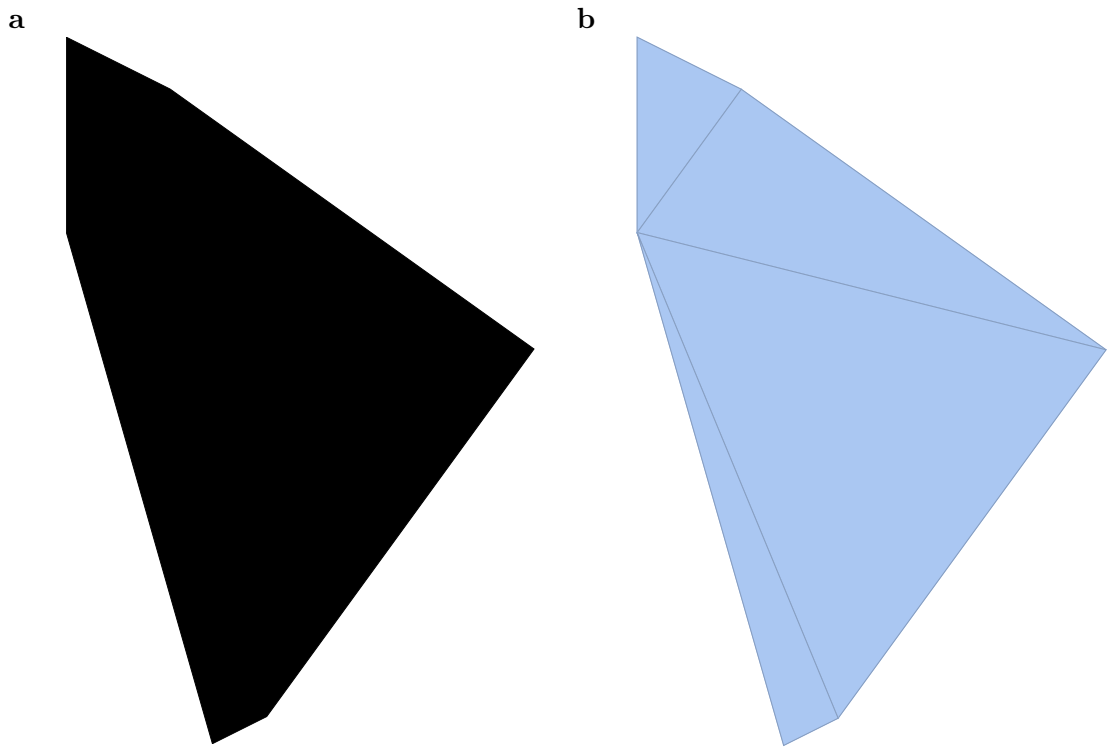

Figure D3: **Triangulating the plane**. Panel (a) shows the shape of the intersection; note that the volume of this region has no direct relationship with the volume of the original overlap. Panel (b) shows the triangulation of the intersection simplex.

E Constraints on intrinsic growth rates

In the majority of feasibility studies, it is assumed that there are no constraints acting on energy flows across trophic levels, i.e., the intrinsic growth rates of different species are independent and can have any possible value. We focus on linear constraints to provide a starting point for addressing this problem, where an analytic description of constraints can be incorporated.

There are two types of linear constraints: linear inequalities and linear equalities. Although they are equivalent by introducing auxiliary variables in the sense of mathematics (Bertsimas & Tsitsiklis, 1997), they have different meanings in ecology. First we focus on linear inequalities. The general form of constraints (lower and upper bounds) on one species i is:

$$L_i \leq r_i \leq U_i. \tag{E1}$$

The most simple example is that the sign of intrinsic growth rates can be fixed (Logofet, 1993); for instance, a given predator and prey may have negative and positive intrinsic growth rates, respectively. Biologically speaking, a finite L_i and U_i exist for any $i \in \{1, ..., S\}$. Thus, we always have the following constraints on equilibrium abundances:

$$L_i \leq \sum_{l=1}^{S} \mathbf{v}_i^l \lambda_l \leq U_i \quad , \quad i = 1, .., S; \tag{E2}$$

$$\lambda_i > 0 \quad , \quad i = 1, ..., S, \tag{E3}$$

where $\mathbf{v}_i^l$ stands for the i-th component of the spanning vector corresponding to species l.

Note that these constraints are in essence different from the overlap of feasibility cones. The feasibility cone is shrinked to a bounded polytope. There is no restraint on its shape (Ball, 1997) except that it is a convex subset of the original feasibility cone. In particular, this cone might be an empty set, which is also another indication of why the structure of intrinsic growth rates is so important. Besides the inequality constraints on one species, it is also common to see equality constraints on the relationship of several species, as metabolic rates may also be similar among species.

With regard to linear equalities, we check the most simple case first. Suppose two species i, j have exactly the same growth rates. This constraint can be written explicitly as

$$\sum_{l=1}^{S} \lambda_l \mathbf{v}_i^l = \sum_{l=1}^{S} \lambda_l \mathbf{v}_j^l. \tag{E4}$$

By denoting $\delta v = (v_i^1 - v_j^1, ..., v_i^S - v_j^S)$ and $\lambda = (\lambda_1, ..., \lambda_S)$, this constraint can be equivalently written as

$$\delta v \cdot \lambda = 0. \tag{E5}$$

Although this constraint seems to be local, it turns out that it introduces a global relationship among abundances of all species. A direct consequence of the constraint (E5) is that the dimension of the sampling space is reduced by 1.

All the reasoning above can be easily generalized to different types of constraints. Consider a constraint $\sum_{k \in T} a_k r_k = 0$ where $a_k \neq 0$ and T is a subset of $\{1, ..., S\}$ whose cardinality is strictly

greater than 1. It would generically pose one linear constraint on λ, which is the cardinality of T. Note that there are only S components of λ, thus generically there cannot be more than S constraints. This is a very important distinction from inequalities.

The computation of a general polyhedra (constraints) in high dimension can be done through a Markov chain Monte Carlo method (Dyer et al., 1991; Jerrum & Sinclair, 1996). It is important to note that the it is time-consuming in high dimension. In the main text, we have focused on the relative volume of the feasible region as it has a natural probabilistic interpretation. However, in many cases, the interests might be on the optimization of some functions of species abundances (Goh, 2012). Because most of convex nonlinear constraints can be efficiently computed (Boyd & Vandenberghe, 2004), this kind of problem can be solved via setting the species growth rates as undetermined parameters. Of course, the optimization of any linear function whose variables are species abundances can be easily computed (Bertsimas & Tsitsiklis, 1997). All the code in R will be archived on Github.